

physica **p** status **s** solidi **s**

www.pss-journals.com

reprint



Stacked structure of self-organized cubic InN nano-dots grown by molecular beam epitaxy

Shuhei Yagi*, Junichiro Suzuki, Misao Orihara, Yasuto Hijikata, and Hiroyuki Yaguchi

Graduate School of Science and Engineering, Saitama University, 255 Shimo-Okubo, Sakura-ku, 338-8570 Saitama, Japan

Received 23 June 2013, accepted 26 August 2013

Published online 30 September 2013

Keywords cubic InN, nano-scale dot, molecular beam epitaxy, scanning transmission electron microscopy

* Corresponding author: e-mail yagi@opt.ees.saitama-u.ac.jp, Phone/Fax: +81 -48-858-3470

A two-stacked cubic (c-) InN/c-GaN nano-scale dot structure is fabricated on a MgO(001) substrate by RF-N₂ molecular beam epitaxy and its microstructures are investigated by scanning transmission electron microscopy (STEM). The cubic lattice structure of InN dots is verified by STEM observations. It is implied that c-InN dots formed on a smooth c-GaN surface have the {111} facets. The c-GaN cap layer has an uneven surface, which re-

flects the shape of the c-InN dots embedded beneath the cap layer. InN selectively deposits in concave regions on the c-GaN cap layer, which appear above in-between positions of embedded dots. Thus, stacked c-InN/c-GaN dots do not tend to align vertically. These results open the possibility for multi-stacking structures of c-InN dots and their application to high-performance optoelectronic devices based on the nitride semiconductors.

© 2013 WILEY-VCH Verlag GmbH & Co. KGaA, Weinheim

1 Introduction Heterostructures based on the InN/(In)GaN system have significant potential for optoelectronic devices such as infrared light emitting devices and multijunction solar cells covering the full range of the solar spectrum [1, 2]. In particular, InN quantum dot based heterostructures have attracted much attention for exploring new phenomena and advanced applications [3]. Strain-induced self-organized growth of nano-scale semiconductor dots is one of the convenient methods to obtain high quality quantum dots with high area density [4-7]. We have recently reported the self-organized growth of nano-scale dots of cubic zincblende phase InN (c-InN) on cubic phase GaN (c-GaN) underlayers by RF-N₂ plasma molecular beam epitaxy (RF-MBE) [8]. Although the cubic phase is metastable for the nitrides, they have several advantages in practical viewpoint compared to nitrides in the hexagonal wurtzite phase. For example, their higher crystalline symmetry of cubic nitrides results in isotropic properties and no spontaneous polarization induced-electric fields in the direction parallel to the c-axis. In addition, it is expected that cubic nitrides have superior electronic properties such as higher carrier mobilities, higher drift velocities and better doping efficiencies [9]. Multiple stacking of quantum dots is an effective way to increase the number of

quantum dots in the active region, and thus, is a key structure for achieving high performance devices. For the fabrication of multiple stacking dot structures, a combination of the dot capping process by the growth of a barrier material and overgrowth of quantum dots on the cap layer provides a basis. Therefore, understanding of the both processes is important. In this study, we have tried to fabricate a two-stacked c-InN/c-GaN dot structure by GaN capping process of c-InN dots and overgrowth of InN on the GaN cap layer. Structural characterization of the stacking structure has been performed by reflection high energy electron diffraction (RHEED), atomic force microscopy (AFM) and scanning transmission electron microscopy (STEM).

2 Experimental Samples were fabricated by RF-MBE on MgO(001) substrates. Before deposition, a MgO substrate was thermally cleaned for 30 minutes at 1100 °C to obtain an atomically flat surface. Then a 15 nm-thick low temperature (LT) GaN buffer layer was grown on the substrate at 550 °C followed by the growth of a c-GaN underlayer with a thickness of 500 nm at 800 °C. After that, InN was deposited to form nano-scale dots at 490 °C with a deposition amount of 4.2 nm. The above procedure provides c-InN dots with an area density of 10¹⁰–10¹¹ cm⁻² [8].

After the dot formation, a GaN cap layer with a thickness of 25 nm was deposited on the surface to encapsulate the c-InN dots while keeping the growth temperature at 490 °C. Finally, fabrication of a stacked c-InN structure was tried by depositing InN again on the GaN cap layer at 490 °C with a deposition amount of 4.2 nm. Surface conditions during and after each stage of the growth process were observed by RHEED and AFM, respectively. Cross-sectional microstructure of the fabricated sample was investigated by STEM.

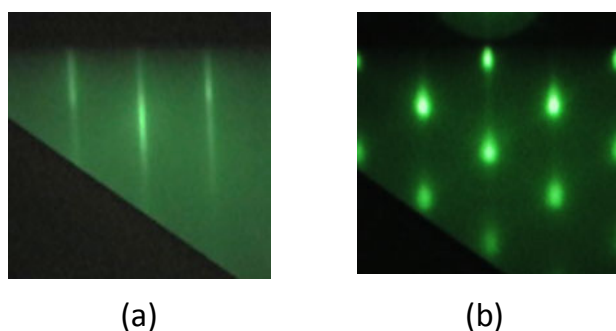


Figure 1 RHEED patterns taken immediately after the deposition of (a) c-GaN underlayer and (b) second InN.

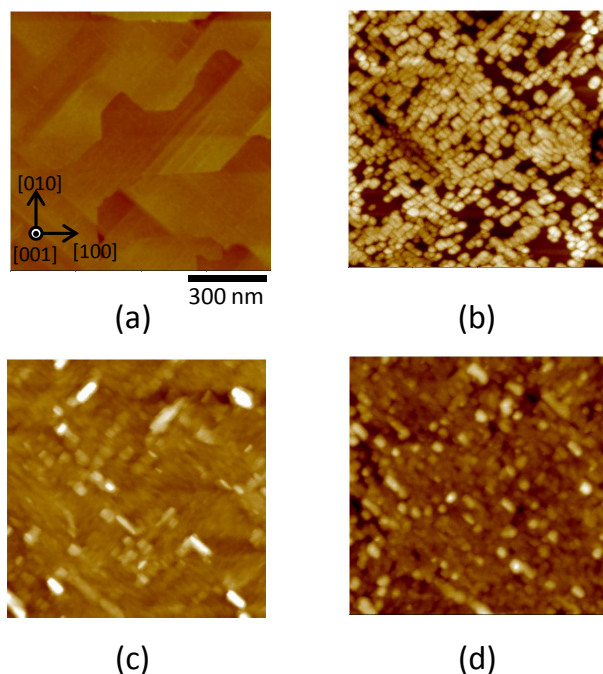


Figure 2 AFM images of the surface at each growth step. (a) c-GaN underlayer, (b) first deposited InN, (c) GaN cap layer and (d) second deposited InN. Scan areas are $1 \times 1 \mu\text{m}^2$.

3 Results and discussion Figures 1 (a) and (b) indicate RHEED patterns taken immediately after the deposition of c-GaN underlayer and second InN, respectively. The pattern obtained from the c-GaN surface showed long streaks indicating the smooth surface of the c-GaN underlayer. The pattern then changed to spots by the following InN deposition, indicating the dot formation. The spotty pattern represented the structural features of the zincblende lattice [10, 11], and was kept throughout the following processes of the GaN cap growth and second InN deposition.

Figure 2 shows AFM images taken after each fabrication step of the stacking structure. The AFM image in Fig. 2(a) with a small root mean square (RMS) roughness of 0.4 nm indicates that an atomically smooth surface of the c-GaN underlayer is obtained. The formation of nano-scale dot structures with a high area density of $\sim 9 \times 10^{10} \text{ cm}^{-2}$ by InN deposition is confirmed from Fig. 2(b). Figure 2(c) shows the surface of the GaN cap layer. As can be observed in the image, an uneven surface seems to reflect the shape of the embedded c-InN dots beneath the cap layer. Figure 2(d) shows the AFM image taken after the second InN deposition. Although the size uniformity of the second dots are degraded compared to the first dots, high density dot structures are observed on the surface.

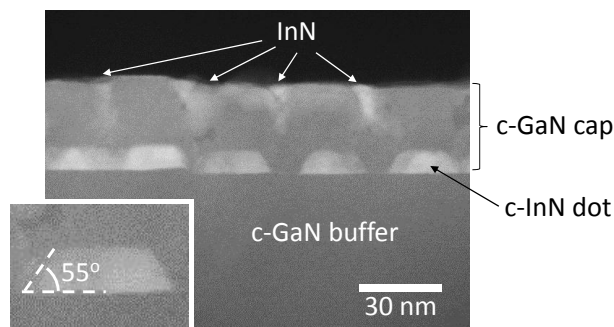


Figure 3 A HAADF-STEM image of the fabricated sample, taken along the [110] zone axis. A number of embedded c-InN dots in the GaN cap layer are clearly observed. A magnified view of an InN dot is indicated at the lower left.

Figure 3 shows a high angle annular dark field (HAADF) STEM image of the fabricated sample taken along the [110] zone axis. A number of c-InN dots with trapezoidal cross-sections embedded in GaN are observed in the image. The width and height of the embedded dots are 25–30 nm and 8–10 nm, respectively. The sharp contrast at the interface between the InN dots and GaN cap layer suggests that no intermixing takes place during the dot formation and capping processes. The base angles of the trapezoids are about 55°, which implies that the side walls of the embedded c-InN dots consist of {111} facets. Figures 4(a) and (b) show transmission electron diffraction (TED) patterns taken from an embedded InN dot and the

GaN cap layer in Fig. 3, respectively. Both of the patterns represent the features of the zincblende structure [10, 11]. Diffraction spots from c-GaN around the dot are slightly overlapped to the pattern of the c-InN dot in Fig. 4(a). The ratio of the lattice constant of the embedded c-InN dot to c-GaN is estimated from the distance between the diffraction spot centres and is about 1.1. This value is in agreement with the ratio of the lattice constants between the bulk crystals of c-InN and c-GaN. This fact indicates that the c-InN dots embedded in the c-GaN matrix are almost unstrained.

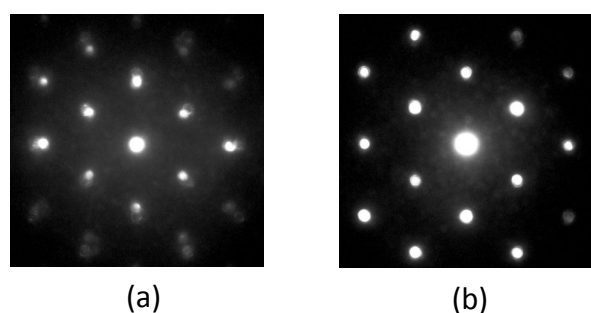


Figure 4 TED patterns taken along [110] zone axis from (a) an embedded c-InN dot and (b) the c-GaN cap layer in Fig. 3. Diffraction spots from c-GaN around the dot are slightly overlapped to the pattern of the c-InN dot in (a).

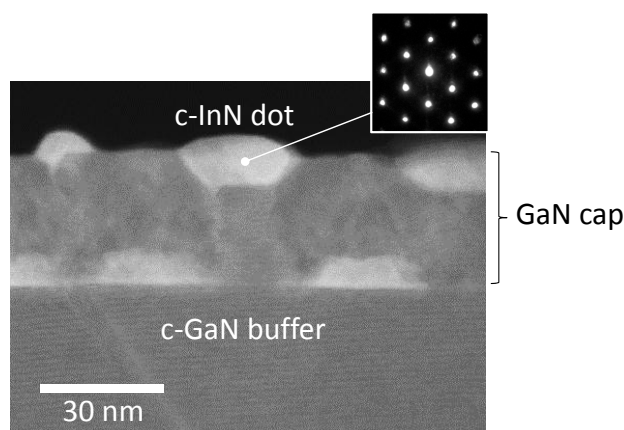


Figure 5 HAADF-STEM image of a stacked structure of InN dots taken along the [110] zone axis. The upper right image is a TED pattern taken from an InN dot formed on the surface of the GaN cap layer.

InN deposited on the c-GaN cap layer is also observed in Fig. 3. An uneven surface of the c-GaN cap layer reflects the shape of the c-InN dots embedded beneath the cap layer, which is consistent with the RHEED and AFM observations. That is, convex regions are formed just above the embedded dots while concave regions are

formed above in-between positions of the embedded dots. As can be seen in the STEM image, InN tends to deposit in the concave regions of the c-GaN cap surface as they are filled with InN.

Some of InN on the c-GaN cap layer forming dot-like shape is found in a STEM image at a different region in the same sample as shown in Fig. 5. Observed TED pattern from a surface InN dot indicates the zincblende lattice structure. Therefore, the formation of a c-InN dot on the GaN cap layer is confirmed. Stacked c-InN/c-GaN dots do not tend to align vertically, which is different from stacking structures of InAs/GaAs dots with relatively thin spacer layers [12]. The shape of the c-InN dots on the cap layer is considerably different from that of the embedded c-InN dots suggesting that different growth mechanism governs the formation of these InN dots.

4 Conclusion A two-stacked c-InN/c-GaN nano-scale dot structure is fabricated on a MgO(001) substrate by RF-MBE. STEM and TED observations verify the cubic lattice structure of embedded and stacked InN dots and the GaN cap layer. It is implied that c-InN dots formed on a smooth c-GaN surface have the {111} facets. The c-GaN cap layer has an uneven surface, which reflects the shape of the c-InN dots embedded beneath the cap layer. InN selectively deposits in concave regions on the c-GaN cap layer, which is different from conventional stacking structures of InAs/GaAs dots, and thus, stacked c-InN/c-GaN dots do not tend to align vertically. These results open the possibility for multi-stacking structures of c-InN dots and their application to high-performance optoelectronic devices based on nitride semiconductors.

Acknowledgements This work is partially supported by Adaptable and Seamless Technology Transfer Program through target-driven R&D (A-STEP) of Japan Science and Technology Agency.

References

- [1] J. Wu, W. Walukiewicz, K. M. Yu, W. Shan, and J. W. Ager III, E. E. Haller, H. Lu, W. J. Schaff, W. K. Metzger, and S. Kurtz, *J. Appl. Phys.* **94**, 6477 (2003).
- [2] R. Dahal, B. Pantha, J. Li, J. Y. Lin, and H. X. Jiang, *Appl. Phys. Lett.* **94**, 063505 (2009).
- [3] Q. Deng, X. Wang, C. Yang, H. Xiao, C. Wang, H. Yin, Q. Hou, J. Li, Z. Wang, and X. Hou, *Physica B* **406**, 73 (2011).
- [4] B. Maleyre, O. Briot, and S. Ruffenach, *J. Cryst. Growth* **269**, 15 (2004).
- [5] E. Dimakis, A. Georgakilas, E. Iliopoulos, K. Tsagaraki, A. Delimitis, Ph. Komninou, H. Kirmse, W. Neumann, M. Androulidaki, and N. T. Pelekanos, *Phys. Status Solidi C* **3**, 3983 (2006).
- [6] W. Ke, S. Lee, S. Chen, C. Kao, W. Houng, C. Wei, and Y. Su, *J. Alloys Compd.* **526**, 119 (2012).
- [7] A. Yoshikawa, N. Hashimoto, N. Kikukawa, S. B. Che, and Y. Ishitani, *Appl. Phys. Lett.* **86**, 153115 (2005).

- [8] J. Suzuki, M. Orihara, S. Yagi, Y. Hijikata, and H. Yaguchi, *J. Cryst. Growth* (in press).
- [9] S. Yoshida, *Physica E* **7**, 907 (2000).
- [10] S. Sanorpim, E. Takuma, H. Ichinose, R. Katayama, and K. Onabe, *Phys. Status Solidi B* **244**, 1769 (2007).
- [11] T. Schupp, T. Meisch, B. Neuschl, M. Feneberg, K. Thonke, K. Lischka, and D. J. As, *Status Solidi C* **8**, 1495 (2011).
- [12] G. S. Solomon, J. A. Trezza, A. F. Marshall, and J. S. Harris Jr., *Phys. Rev. Lett.* **76**, 952 (1996).